

# Effect of calcination conditions on the species formed and the reduction behavior of the cobalt–magnesia catalysts

E. Ruckenstein\* and H.Y. Wang

Department of Chemical Engineering, State University of New York at Buffalo, Amherst, NY 14260, USA  
E-mail: feaeliru@acsu.buffalo.edu

Received 20 July 2000; accepted 25 September 2000

The structural characteristics and the reduction behavior of the Co/MgO catalysts were investigated using temperature-programmed reduction (TPR) and X-ray diffraction (XRD). The variables investigated included the preparation method and the heat treatment conditions (calcination temperature and time). Depending on these factors, one, two or three of the following Co-containing species,  $\text{Co}_3\text{O}_4$ ,  $\text{MgCo}_2\text{O}_4$  and (Co, Mg)O (solid solution of CoO and MgO) were identified. The extent of solid solution formation increased as the calcination temperature and calcination time increased. A much lower calcination temperature was needed to form a solid solution in the impregnated catalysts than in the physically mixed ones. The formation of a solid solution rendered the catalyst less reducible. Finally, the decomposition of  $\text{CH}_4$ , as a probe reaction, was performed and it was found that the amount of carbon deposited decreased with increasing extent of solid solution formation.

**Keywords:** TPR (temperature-programmed reduction), XRD (X-ray diffraction), Co catalyst, solid solution

## 1. Introduction

To prevent the occurrence of any further solid-state reactions during the catalytic reaction, the supported catalysts are often subjected to calcination at a temperature (usually) higher than the reaction temperature. The solid reactions that occur between the active phase (or its precursor) and support during calcination generally affect the surface and structure of the catalyst and hence its catalytic performance. When transition metal ions can be incorporated into the matrix of the support, solid solutions are formed. In this regard, CoO–MgO constitutes an interesting system, since an ideal solid solution over the whole molar fraction range can be generated [1,2], and Co is an active metal for a number of reactions, such as hydrotreating [3a] and steam reforming [3b] as well as Fischer–Tropsch synthesis [3c].

Recently, we [4] found that Co supported on MgO is a better catalyst for the  $\text{CO}_2$ -reforming of  $\text{CH}_4$  than supported on other oxides such as CaO, SrO, BaO,  $\gamma\text{-Al}_2\text{O}_3$  and  $\text{SiO}_2$ . The former exhibited a high and stable activity under a high space velocity and high reaction temperature (900 °C). The higher performance of this catalyst was related to the formation of a solid solution after a high-temperature calcination. The formation of a solid solution has a number of advantages. Firstly, due to the low reducibility of the solid solution, small clusters of metallic Co are generated. Since coke formation requires relatively large ensembles of sites [5], its generation is thus largely avoided. Secondly, being generated from a solid solution, the clusters acquire the form of hillocks protruding from the substrate, which

are partially embedded in the substrate; this lessens the sintering of the metallic sites.

Generally, the formation of a solid solution and the distribution of a metal oxide inside the support are expected to depend on the initial dispersion of the metal oxide (or its precursor) over the support and the migration of metal ions inside the support during the heat treatment. While the former is closely dependent on the preparation method, the latter is strongly affected by the heat treatment conditions. Hence, it is of interest to investigate the structural characteristics and the reduction behavior of the MgO-supported Co catalysts, prepared by various methods, as a function of calcination temperature and calcination time.

## 2. Experimental

### 2.1. Catalyst preparation

Two methods, impregnation and physical mixing, were used to prepare the catalysts. In the first method, MgO (32  $\text{m}^2/\text{g}$ ) was impregnated with an aqueous solution of  $\text{Co}(\text{NO}_3)_2 \cdot 6\text{H}_2\text{O}$ , followed by overnight drying at 110 °C. In the second, predetermined amounts of MgO and CoO powders were mixed in an ethanol solution, followed by overnight drying at 110 °C. The obtained samples were then calcined in the open air of a furnace for 8 h (unless otherwise indicated), at various temperatures ranging between 300 and 1000 °C. The calcined catalysts prepared by impregnation are denoted wt% Co(O)/MgO(Im)(300, 400, ... or 1000 °C), and those prepared by physical mixing wt% Co(O)–MgO(PM)(300, 400, ... or 1000 °C). The temperature inside the parentheses indicates the calcination temper-

\* To whom correspondence should be addressed.

ature and wt% Co(O) indicates wt% Co in the completely reduced catalyst.

## 2.2. Temperature-programmed reduction (TPR)

TPR measurements were performed in a conventional linear quartz microreactor (I.D. 4 mm), using a high-purity flow of a 2.5% H<sub>2</sub>/Ar mixture (35 ml/min), which was additionally purified with Hydro-Purge II and Oxy-Trap columns. During each TPR run, the reducing mixture was passed over a calcined sample (10.0 mg, unless otherwise indicated), held on a quartz wool bed in the reactor. The temperature of the sample was increased from 40 to 1000 °C, at a rate of 20 °C/min. The water formed during reduction was trapped in a Hydro-Purge II column. The hydrogen consumed in TPR was monitored continuously with a thermal conductivity detector (TCD), which was calibrated using known amounts of CoO and Co<sub>3</sub>O<sub>4</sub>.

## 2.3. X-ray powder diffraction (XRD)

XRD determinations were carried out using a Siemens D500 X-ray diffractometer instrument with a Cu K $\alpha$  radiation at 40 kV and 30 mA. The lattice parameters ( $a$ ) of MgO, CoO–MgO solid solution and CoO were calculated from the diffractions of the (200) face, and those of Co<sub>3</sub>O<sub>4</sub> and Co<sub>2</sub>MgO<sub>4</sub> of the (440) face, using the equation

$$a = (h^2 + k^2 + l^2)^{1/2} \lambda / (2 \sin \theta), \quad (1)$$

where  $\lambda$  is the wave length and  $\theta$  the diffraction angle. The extent of CoO dissolution into the MgO lattice was estimated from the value of the lattice parameter ( $a$ ) assuming a linear variation of  $a$  between 4.2111 and 4.2530 Å, which

represent the lattice parameters of pure MgO and CoO, respectively.

## 2.4. CH<sub>4</sub> decomposition

The decomposition of pure methane over the reduced 24 wt% Co/MgO(Im) catalyst was carried out in a pulse microreactor, consisting of a quartz tube (I.D. 4 mm), in which the calcined catalyst (50.0 mg) was held on a quartz wool bed. The reduction was carried out in a H<sub>2</sub> flow (20 ml/min), by increasing the temperature from room temperature to 600 °C at a rate of 20 °C/min and then to 900 °C at a rate of 10 °C/min, without holding at 900 °C. After reduction, the catalyst was purged with the carrier gas He (35 ml/min) at 900 °C for 0.25 h, and then pulses of CH<sub>4</sub> (250  $\mu$ l) were injected in the carrier gas. The products were analyzed with an on-line gas chromatograph equipped with a TCD and a Porapak Q column.

## 3. Results and discussion

The purpose of the present investigation was to identify the various Co-containing species formed, to estimate the extent of solid solution generated, and to evaluate the degree of reduction of the cobalt–magnesia catalysts. The variables investigated included the preparation method and the heat treatment conditions (calcination temperature and time). TPR was the main technique employed. The values of  $T_m$  (the temperature of a TPR peak maximum) and of the degree of reduction (calculated from the H<sub>2</sub> consumption) are listed in tables 1 and 2. XRD was used as a supplementary technique on some of the catalysts to identify the

Table 1  
Temperature-programmed reduction of cobalt oxides, Co(O)–MgO(PM) and Co(O)/MgO(Im) catalysts.

Sample	$T_m^a$ (°C)			Degree of reduction (%)
	Region I	Region II	Region III	
CoO <sup>b</sup>	392	–	–	~100
Co <sub>3</sub> O <sub>4</sub> <sup>c</sup>	404	–	–	~100
24 wt% Co(O)–MgO(PM)(300 °C)	356	–	–	66
24 wt% Co(O)–MgO(PM)(400 °C)	348	–	–	77
24 wt% Co(O)–MgO(PM)(500 °C)	356	–	–	93
24 wt% Co(O)–MgO(PM)(600 °C)	364	–	–	~100
24 wt% Co(O)–MgO(PM)(700 °C)	364	–	–	92
24 wt% Co(O)–MgO(PM)(800 °C)	340	–	–	58
24 wt% Co(O)–MgO(PM)(900 °C)	328	–	–	22
24 wt% Co(O)–MgO(PM)(1000 °C)	–	–	>1000	4
24 wt% Co(O)/MgO(Im)(300 °C)	312	672	–	65
24 wt% Co(O)/MgO(Im)(400 °C)	292	688	–	
24 wt% Co(O)/MgO(Im)(500 °C)	300	660	–	24
24 wt% Co(O)/MgO(Im)(600 °C)	298, 430	–	–	
24 wt% Co(O)/MgO(Im)(700 °C)	400	–	>1000	19
24 wt% Co(O)/MgO(Im)(800 °C)	–	–	>1000	3
24 wt% Co(O)/MgO(Im)(900 °C)	–	–	>1000	1

<sup>a</sup> Region I < 500 °C, 500 °C < region II < 800 °C, region III > 800 °C.

<sup>b</sup> 4.2 mg.

<sup>c</sup> 3.4 mg.

species formed. The data and the assignments are listed in tables 3–5.

Typical TPR profiles for (a) pure MgO, (b) pure CoO, (c) pure Co<sub>3</sub>O<sub>4</sub>, (d) 24 wt% Co(O)–MgO(PM)(300 °C), and (e) 24 wt% Co(O)/MgO(Im)(300 °C) are presented in figure 1. MgO did not consume any hydrogen under the experimental conditions employed. CoO and Co<sub>3</sub>O<sub>4</sub> had comparable reduction temperatures; a single reduction peak at 392 °C was observed for CoO, and at 404 °C for Co<sub>3</sub>O<sub>4</sub>.

Table 2  
Effect of calcination time on the reducibility of 48 wt% Co(O)/MgO(Im)(900 °C) catalyst.

$t_c$ (min)	$T_m^a$ (°C)			Degree of reduction (%)
	Region I	Region II	Region III	
0	368	–	>1000	17
2	356	–	>1000	12
5	360	–	>1000	9
30	300	–	>1000	8
180	–	–	>1000	6
480	–	–	>1000	6

<sup>a</sup> Region I < 500 °C, 500 °C < region II < 800 °C, region III > 800 °C.

Table 3  
Data and assignments of XRD patterns of calcined Co(O)/MgO catalysts.

Sample	$d$ (Å)	Possible assignments	Final assignments <sup>a</sup>
24 wt% Co(O)–MgO(PM)(600 °C, 8 h)	2.4355, 1.4295, 2.8531, 1.5558, 2.0230; 2.1056, 1.4897, 1.2151, 1.2699, 2.4355	Co <sub>3</sub> O <sub>4</sub> and/or Co <sub>2</sub> MgO <sub>4</sub> ; (Co, Mg)O and/or MgO	Co <sub>3</sub> O <sub>4</sub> ; MgO
24 wt% Co(O)–MgO(PM)(800 °C, 8 h)	2.4363, 1.4290, 2.8580, 1.5559, 2.0190; 2.1073, 1.4899, 1.2172, 1.2708, 2.4363	Co <sub>3</sub> O <sub>4</sub> and/or Co <sub>2</sub> MgO <sub>4</sub> ; (Co, Mg)O and/or MgO	Co <sub>3</sub> O <sub>4</sub> ; (Co, Mg)O, MgO
24 wt% Co(O)–MgO(PM)(1000 °C, 8 h)	2.1087, 1.4912, 2.4361, 1.2174, 1.2711	(Co, Mg)O and/or MgO	(Co, Mg)O, MgO
24 wt% Co(O)/MgO(Im)(300 °C, 8 h)	2.4440, 1.4345, 2.8649, 1.5696, 2.0247; 2.1065, 1.4891, 2.4400	Co <sub>3</sub> O <sub>4</sub> and/or Co <sub>2</sub> MgO <sub>4</sub> ; (Co, Mg)O and/or MgO	Co <sub>3</sub> O <sub>4</sub> , Co <sub>2</sub> MgO <sub>4</sub> ; (Co, Mg)O, MgO
24 wt% Co(O)/MgO(Im)(700 °C, 8 h)	2.4356, 1.4305, 2.8590, 1.5574, 2.0203; 2.1078, 1.4907, 1.2177, 1.2712, 2.4356	Co <sub>3</sub> O <sub>4</sub> and/or Co <sub>2</sub> MgO <sub>4</sub> ; (Co, Mg)O and/or MgO	Co <sub>3</sub> O <sub>4</sub> ; (Co, Mg)O, MgO
24 wt% Co(O)/MgO(Im)(800 °C, 8 h)	2.1103, 1.4926, 2.4378, 1.2183, 1.2723	(Co, Mg)O and/or MgO	(Co, Mg)O, MgO
48 wt% Co(O)/MgO(Im)(900 °C, 0 h)	2.4410, 1.4302, 2.8604, 1.5570, 2.0209; 2.1135, 1.4949, 1.2215, 1.2749, 2.4410	Co <sub>3</sub> O <sub>4</sub> and/or Co <sub>2</sub> MgO <sub>4</sub> ; (Co, Mg)O and/or MgO	Co <sub>3</sub> O <sub>4</sub> ; (Co, Mg)O, MgO
48 wt% Co(O)/MgO(Im)(900 °C, 8 h)	2.1154, 1.4960, 2.4433, 1.2223, 1.2766	(Co, Mg)O and/or MgO	(Co, Mg)O, MgO

<sup>a</sup> Final assignments were made based on the calculated values of the lattice parameters (see tables 4 and 5).

Table 4  
Lattice parameters calculated from the diffractions of the (200) face.

Sample	$2\theta$ (°)	$a$ (Å)	Composition of MgO-based CoO–MgO solid solution
MgO	42.919	4.2111	MgO
24 wt% Co(O)–MgO(PM)(600 °C, 8 h)	42.917	4.2112	MgO
24 wt% Co(O)–MgO(PM)(800 °C, 8 h)	42.881	4.2145	Co <sub>0.08</sub> Mg <sub>0.92</sub> O
24 wt% Co(O)–MgO(PM)(1000 °C, 8 h)	42.850	4.2174	Co <sub>0.15</sub> Mg <sub>0.85</sub> O
24 wt% Co(O)/MgO(Im)(300 °C, 8 h)	42.896	4.2131	Co <sub>0.05</sub> Mg <sub>0.95</sub> O
24 wt% Co(O)/MgO(Im)(700 °C, 8 h)	42.869	4.2157	Co <sub>0.11</sub> Mg <sub>0.89</sub> O
24 wt% Co(O)/MgO(Im)(800 °C, 8 h)	42.816	4.2206	Co <sub>0.23</sub> Mg <sub>0.77</sub> O
48 wt% Co(O)/MgO(Im)(900 °C, 0 h)	42.748	4.2270	Co <sub>0.38</sub> Mg <sub>0.62</sub> O
48 wt% Co(O)/MgO(Im)(900 °C, 8 h)	42.797	4.2224	Co <sub>0.47</sub> Mg <sub>0.53</sub> O
CoO	42.474	4.2530	CoO

While the 24 wt% Co(O)–MgO(PM)(300 °C) provided a single peak at 356 °C, the 24 wt% Co(O)/MgO(Im)(300 °C) exhibited two peaks, one at 312 °C and the other at 624 °C. As it will be shown in detail later, more complex interactions occur between cobalt and magnesium oxides in the latter case.

### 3.1. Effect of calcination temperature ( $T_c$ )

#### 3.1.1. The 24 wt% Co(O)–MgO(PM) catalysts

The TPR profiles of the 24 wt% Co(O)–MgO(PM) catalysts calcined at different temperatures ranging from 300 to 1000 °C are presented in figure 2. The TPR patterns and the degree of reduction are strongly affected by the calcination temperature. A single reduction peak between 320 and 370 °C was observed for the 24 wt% Co(O)–MgO(PM) catalysts calcined between 300 and 900 °C. For the 24 wt% Co(O)–MgO(PM)(1000 °C) catalyst, a reduction peak started to form at a temperature higher than 800 °C. As shown in figure 3, the degree of reduction increased with increasing calcination temperature  $T_c$  from 300 to 600 °C, but decreased with a further increase in  $T_c$ .

Table 5  
Lattice parameters calculated from the diffractions of the (440) face.

Sample	$2\theta$ ( $^{\circ}$ )	$a$ ( $\text{\AA}$ )	Assignments
$\text{Co}_3\text{O}_4$		8.0840 <sup>a</sup>	
24 wt% $\text{Co(O)-MgO(PM)}$ (600 $^{\circ}\text{C}$ , 8 h)	65.212	8.0863	$\text{Co}_3\text{O}_4$
24 wt% $\text{Co(O)-MgO(PM)}$ (800 $^{\circ}\text{C}$ , 8 h)	65.237	8.0835	$\text{Co}_3\text{O}_4$
24 wt% $\text{Co(O)/MgO(Im)}$ (300 $^{\circ}\text{C}$ , 8 h)	64.957	8.1145	$\text{Co}_3\text{O}_4$ , $\text{Co}_2\text{MgO}_4$
24 wt% $\text{Co(O)/MgO(Im)}$ (700 $^{\circ}\text{C}$ , 8 h)	65.160	8.0920	$\text{Co}_3\text{O}_4$
48 wt% $\text{Co(O)/MgO(Im)}$ (900 $^{\circ}\text{C}$ , 0 h)	65.173	8.0906	$\text{Co}_3\text{O}_4$
$\text{Co}_2\text{MgO}_4$		8.1230 <sup>a</sup>	

<sup>a</sup> Taken from XRD database.

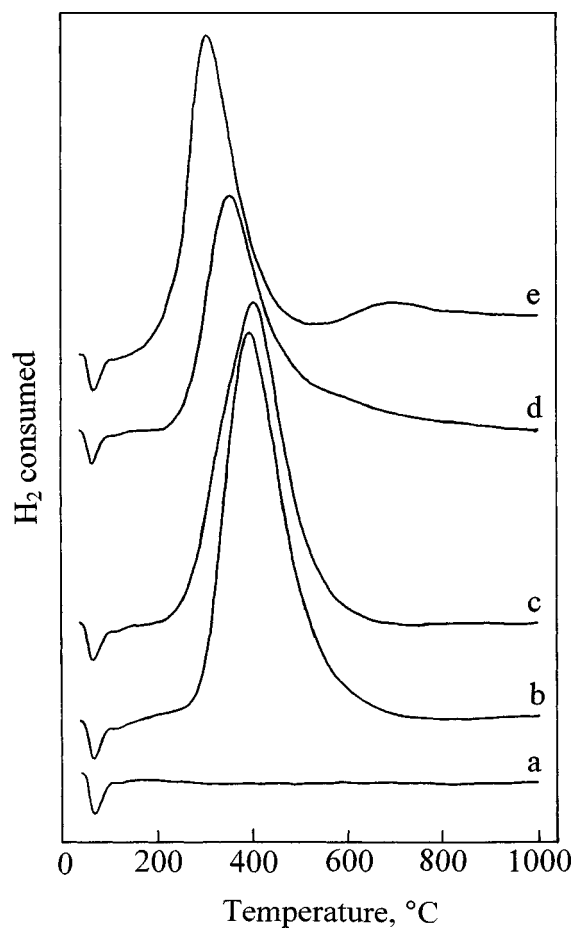


Figure 1. TPR profiles of (a)  $\text{MgO}$ , (b)  $\text{CoO}$ , (c)  $\text{Co}_3\text{O}_4$ , (d) 24 wt%  $\text{Co(O)-MgO(PM)}$ (300  $^{\circ}\text{C}$ ) and (e) 24 wt%  $\text{Co(O)/MgO(Im)}$ (300  $^{\circ}\text{C}$ ) (attenuation value for GC: 64).

Only at the  $T_c$  of 600  $^{\circ}\text{C}$ , an almost complete reduction was reached.

The XRD patterns for the 600  $^{\circ}\text{C}$  calcined catalyst could be assigned to  $\text{Co}_3\text{O}_4$  and/or  $\text{Co}_2\text{MgO}_4$ , as well as to  $(\text{Co,Mg})\text{O}$  and/or  $\text{MgO}$  (table 3) (the X-ray patterns for  $\text{Co}_3\text{O}_4$  and  $\text{Co}_2\text{MgO}_4$  are very similar, and those of  $(\text{Co,Mg})\text{O}$  and  $\text{MgO}$  are also very similar). The lattice parameters calculated from the diffractions of (200) and (440) faces were 4.2112 and 8.0863  $\text{\AA}$  (tables 4 and 5), which are very close to those of  $\text{MgO}$  and  $\text{Co}_3\text{O}_4$ , respectively. Hence, the above calculations suggested that  $\text{Co}_3\text{O}_4$

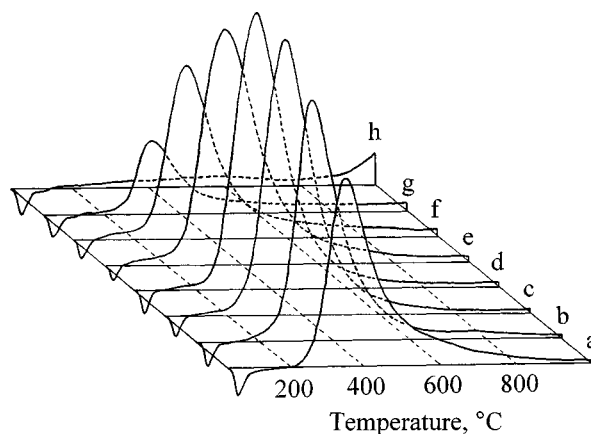


Figure 2. TPR profiles of 24 wt%  $\text{Co(O)-MgO(PM)}$  catalysts precalcined at (a) 300, (b) 400, (c) 500, (d) 600, (e) 700, (f) 800, (g) 900 and (h) 1000  $^{\circ}\text{C}$  (attenuation value for GC: 64).

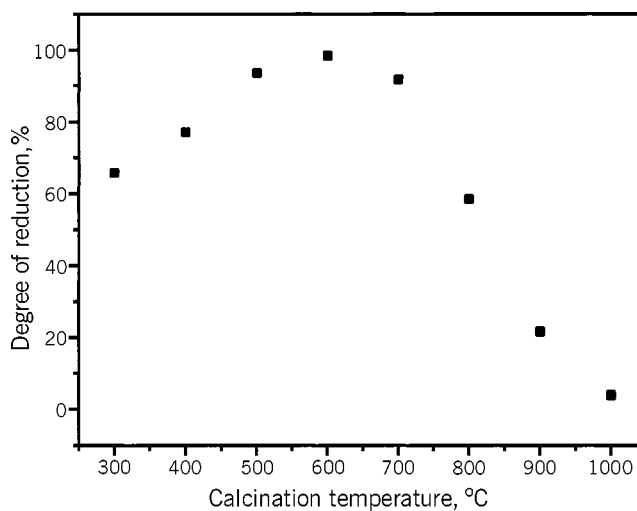


Figure 3. Effect of calcination temperature on the reducibility of 24 wt%  $\text{Co(O)-MgO(PM)}$  catalysts.

and  $\text{MgO}$  were present in that specimen. This conclusion is in agreement with the TPR results, which exhibited a single reduction peak at 364  $^{\circ}\text{C}$  (figure 2(d)) (which can be attributed to  $\text{Co}_3\text{O}_4$ ) and a 100% degree of reduction (table 1). Similarly, the XRD results for the 800  $^{\circ}\text{C}$  calcined catalyst indicated the presence of  $\text{Co}_3\text{O}_4$  and  $(\text{Co,Mg})\text{O}$  (tables 3–5). Even though only a single peak at 340  $^{\circ}\text{C}$  (which can be attributed to  $\text{Co}_3\text{O}_4$ ) was observed in the

TPR spectrum (figure 2(f)), the relatively low (58%) degree of reduction reached implied the presence of a solid solution. The absence of a TPR peak for the solid solution is most likely due to the insufficiently high upper-limit temperature in the TPR experiment. Finally, the XRD results for the 1000 °C calcined catalyst indicated the presence of (Co,Mg)O (tables 3–5). This is in agreement with the TPR spectrum, which exhibited a peak that started to be formed at a temperature >800 °C (figure 2(h)).

Since the formation of a solid solution is a temperature-activated process and no solid solution was present in the 600 °C calcined catalyst, no solid solution could have been generated for the catalysts calcined at a temperature <600 °C. The incomplete reduction observed for the latter catalysts was most likely due to the incomplete reduction of  $\text{Co}_3\text{O}_4$ . On the basis of the above results and the TPR spectra, it is reasonable to conclude that solely  $\text{Co}_3\text{O}_4$  was present as a Co-containing species in the catalysts calcined at  $\leq 600$  °C, both  $\text{Co}_3\text{O}_4$  and (Co,Mg)O in the catalysts calcined between 700 and 900 °C, and only (Co,Mg)O in the 1000 °C calcined catalyst.

The maximum of the degree of reduction as a function of  $T_c$  (figure 3) can be explained as follows. For  $T_c < 600$  °C, Co was present solely as  $\text{Co}_3\text{O}_4$  and its dispersion over the surface of the support increased, because of wetting, with increasing  $T_c$ . The increase in the reduction degree was due to the larger area accessible to  $\text{H}_2$ . For  $T_c > 600$  °C, a solid solution, which is less reducible than  $\text{Co}_3\text{O}_4$ , started to be formed and its amount increased with increasing  $T_c$ . Indeed, for  $T_c > 600$  °C, the area underneath the TPR peak corresponding to  $\text{Co}_3\text{O}_4$  decreased (figure 2) and the Co concentration as (Co,Mg)O increased (table 4) with increasing  $T_c$ . For a  $T_c$  of 1000 °C, a complete solid solution was formed, which provided the lowest reduction degree.

### 3.1.2. 24 wt% Co(O)/MgO(Im) catalysts

The TPR profiles of the 24 wt% Co(O)/MgO(Im) catalysts calcined at different temperatures ranging from 300 to 900 °C are presented in figure 4. The 24 wt% Co(O)/MgO(Im)(300 °C) exhibited two reduction peaks, one at 312 °C and the other at 672 °C. The reduction degree of the sample was 65%, which is much smaller than 100%. When  $T_c$  was increased to 400 °C, the intensity of the first reduction peak decreased tremendously (in contrast with what was observed for the Co(O)–MgO(PM) catalysts), while that of the second reduction peak increased to some extent. It is obvious that the degree of reduction decreased compared to that at 300 °C. No obvious changes were observed when  $T_c$  was increased from 400 to 500 °C. With a further increase in  $T_c$  to 600 °C, the second peak was shifted to a lower temperature (from 660 to 430 °C). At  $T_c = 700$  °C, in addition to a wide single peak at 400 °C, a peak started to form at a temperature higher than 800 °C. For the calcination temperatures of 800 and 900 °C, only a single peak started to form at temperatures higher than 800 °C. The de-

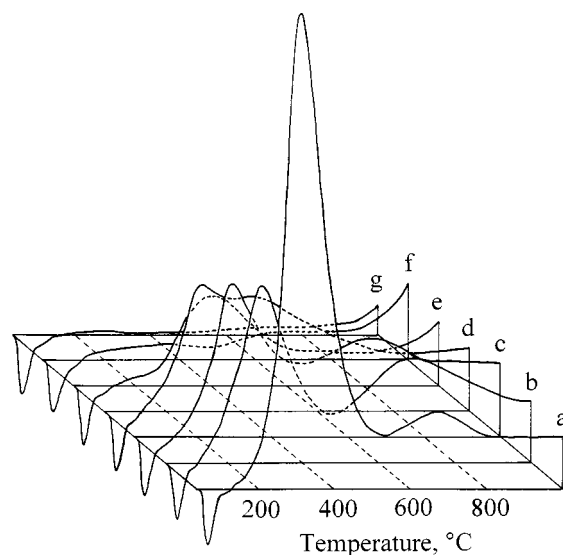


Figure 4. TPR profiles of 24 wt% Co(O)/MgO(Im) catalysts precalcined at (a) 300, (b) 400, (c) 500, (d) 600, (e) 700, (f) 800 and (g) 900 °C (attenuation value for GC: 32).

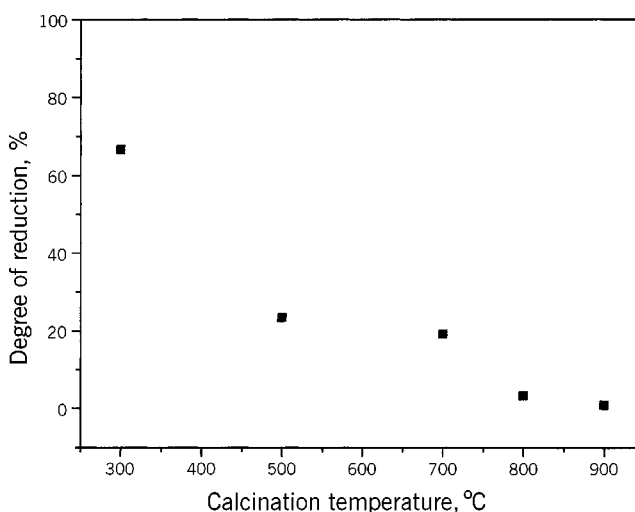


Figure 5. Effect of calcination temperature on the reducibility of 24 wt% Co(O)/MgO(Im) catalysts.

gree of reduction decreased monotonically with increasing calcination temperature  $T_c$  from 300 to 900 °C (figure 5).

The XRD results for the 300 °C calcined catalyst indicated the presence of  $\text{Co}_3\text{O}_4$ ,  $\text{Co}_2\text{MgO}_4$  and (Co,Mg)O (tables 3–5). Because the reducibility decreases in the sequence  $\text{Co}_3\text{O}_4 > \text{Co}_2\text{MgO}_4 > (\text{Co,Mg})\text{O}$ , and the reduction of  $\text{Co}_3\text{O}_4$  occurs below 500 °C and that of (Co,Mg)O requires a temperature >800 °C, the TPR peaks at 312 and at 672 °C (figure 4(a)) can be attributed to  $\text{Co}_3\text{O}_4$  and  $\text{Co}_2\text{MgO}_4$ , respectively. The relatively low (65%) degree of reduction provided an additional indication for the presence of a solid solution. The absence of a TPR peak for the solid solution is due to the insufficiently high upper-limit temperature in the TPR experiment. Similarly, the XRD results for the 700 °C calcined catalyst indicated the presence of  $\text{Co}_3\text{O}_4$  and (Co,Mg)O (tables 3–5). This is



in agreement with the TPR spectrum, which exhibited two peaks, one at 400 °C and another one that started to form at a temperature higher than 800 °C (figure 4(e)). Finally, the XRD results for the 800 °C calcined catalyst indicated the presence of (Co,MgO)O as the only Co-containing species (tables 3–5). This is again in agreement with the TPR spectrum (figure 4(f)). On the basis of the above results and the TPR spectra, one can conclude that  $\text{Co}_3\text{O}_4$ ,  $\text{Co}_2\text{MgO}_4$  and (Co,Mg)O were present in the catalysts calcined between 300 and 600 °C,  $\text{Co}_3\text{O}_4$  and (Co,Mg)O in the 700 °C calcined catalyst, and solely (Co,Mg)O in the catalysts calcined at temperatures  $\geq 800$  °C. The Co concentration in the solid solution increased from  $\text{Co}_{0.05}\text{Mg}_{0.95}\text{O}$  to  $\text{Co}_{0.23}\text{Mg}_{0.77}\text{O}$  with increasing  $T_c$  from 300 to 800 °C (table 4). Thus, a higher calcination temperature promoted the formation of a solid solution through the diffusion of CoO into the MgO lattice.

The reducibility of the Co-containing species decreases in the sequence  $\text{Co}_3\text{O}_4 > \text{Co}_2\text{MgO}_4 > (\text{Co,Mg})\text{O}$ . Hence, the reducibility of the catalyst is directly related to the species present. For conditions that favor the formation of a solid solution, the percentage of cobalt that can be reduced to the metal is decreased. Indeed, due to the formation of a solid solution and the diffusion of CoO into MgO, which are enhanced by increasing  $T_c$ , the reducibility of the catalysts monotonically decreased over the Co(O)/MgO(Im) catalysts (figure 5).

### 3.1.3. Comparison between the Co(O)/MgO(Im) and Co(O)–MgO(PM) catalysts

For both 24 wt% catalysts, prepared by impregnation and physical mixing, the species formed and the diffusion of CoO into MgO during calcination were strongly dependent on  $T_c$ . At high values of  $T_c$ , complete solid solutions were formed in both cases. However, there are notable differences between the two at lower calcination temperatures. One or two of the species,  $\text{Co}_3\text{O}_4$  and (Co,Mg)O, were identified in the Co(O)–MgO(PM) catalysts, while one, two or three of the species,  $\text{Co}_3\text{O}_4$ ,  $\text{Co}_2\text{MgO}_4$  and (Co,Mg)O, in the Co(O)/MgO(Im) catalysts. The  $T_c$  needed to form a solid solution was much lower for the Co(O)/MgO(Im) catalysts than for the Co(O)–MgO(PM) ones. At the same  $T_c$ , the solid solution had a higher Co concentration for Co(O)/MgO(Im) than for Co(O)–MgO(PM) (at 800 °C, they were  $\text{Co}_{0.23}\text{Mg}_{0.77}\text{O}$  and  $\text{Co}_{0.08}\text{Mg}_{0.92}\text{O}$ , respectively). Consequently, the impregnated catalysts had a stronger propensity to form a solid solution than the physically mixed ones. These differences were most likely caused by the different initial dispersions of CoO (or its precursor) over the support, which affected the diffusion of  $\text{Co}^{2+}$  during calcination. Obviously, a higher dispersion over the MgO surface was achieved with the impregnated catalysts.

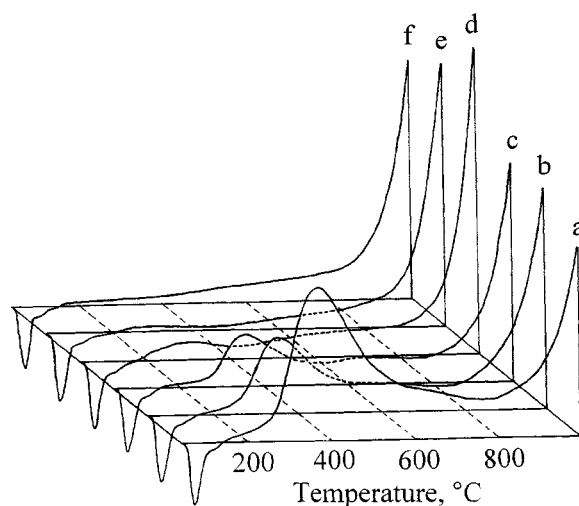


Figure 6. TPR profiles of 48 wt% Co(O)/MgO(Im) catalysts precalcined by increasing the temperature from room temperature to 900 °C and holding at 900 °C for (a) 0, (b) 2, (c) 5, (d) 30, (e) 180 and (f) 480 min (attenuation value for GC: 32).

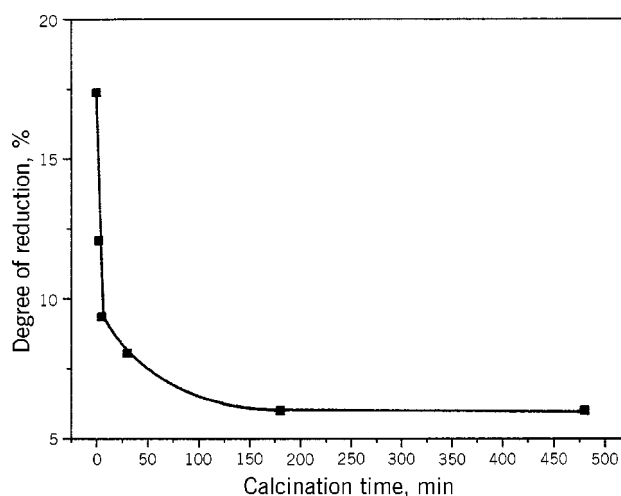


Figure 7. Effect of calcination time on the reducibility of 48 wt% Co(O)/MgO(Im)(900 °C) catalysts.

### 3.2. Effect of calcination time ( $t_c$ )

The TPR profiles of the 48 wt% Co(O)/MgO(Im) catalysts calcined at 900 °C for various times are presented in figure 6. The catalyst, calcined by increasing the temperature from room temperature to 900 °C without holding at 900 °C, exhibited two TPR peaks, one at 368 °C and another one that started to form at a temperature higher than 800 °C (figure 6(a)). They could be attributed to  $\text{Co}_3\text{O}_4$  and (Co,Mg)O, respectively. This is in agreement with the XRD results (tables 3–5), which also suggested the presence of  $\text{Co}_3\text{O}_4$  and (Co,Mg)O. With increasing calcination time  $t_c$ , the peak corresponding to  $\text{Co}_3\text{O}_4$  became increasingly smaller and disappeared for  $t_c = 8$  h. For the catalyst calcined for 8 h at 900 °C, the XRD results indicated that solely (Co,Mg)O was present as a Co-containing species. The relationship between the degree of reduction and  $t_c$  is presented in figure 7. The degree of reduction decreased

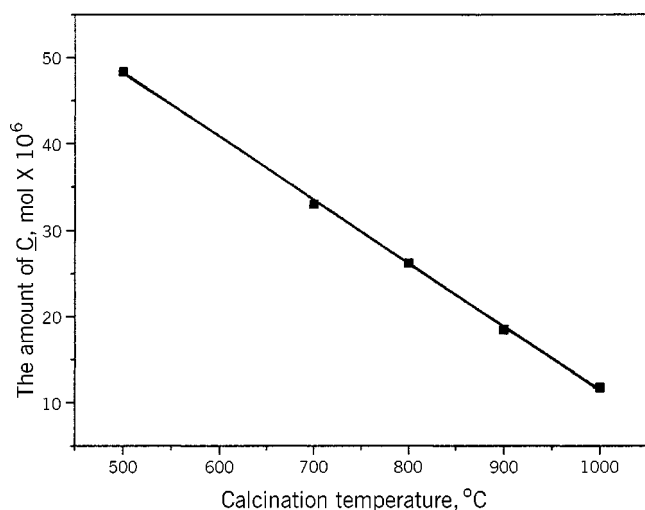


Figure 8. The amount of carbon deposited ( $\bar{C}$ ) in the first 20 pulses of  $\text{CH}_4$  as a function of calcination temperature, in  $\text{CH}_4$  decomposition at  $900^\circ\text{C}$  over the reduced 24 wt% Co/MgO(Im) catalysts.

greatly during the first 0.5 h and then moderately, until a steady state was reached. The results indicated that the decomposition of  $\text{Co}_3\text{O}_4$  and the diffusion of CoO into the MgO matrix occurred, which were enhanced by increasing  $t_c$  until a quasi-steady state was reached. As shown in table 3, the 48 wt% Co(O)/MgO(Im) catalysts calcined at  $900^\circ\text{C}$  for 0 and 8 h had the compositions  $\text{Co}_{0.38}\text{Mg}_{0.62}\text{O}$  and  $\text{Co}_{0.47}\text{Mg}_{0.53}\text{O}$ , respectively.

### 3.3. Decomposition of $\text{CH}_4$ over the 24 wt% Co/MgO(Im) catalysts

The decomposition of  $\text{CH}_4$  over the 24 wt% Co/MgO(Im) catalysts was studied in a pulse microreactor at  $900^\circ\text{C}$ . Figure 8 presents the amount of carbon deposited ( $\bar{C}$ ) during the first 20 pulses of  $\text{CH}_4$  as a function of the calcination temperature  $T_c$ . It decreased linearly with increasing  $T_c$ . As noted earlier, due to the formation of a solid solution between CoO and MgO, which was stimulated by higher values of  $T_c$ , the reducibility of the catalyst decreased. Consequently, the amount of metallic sites and the size of the

metal particles became increasingly smaller with increasing  $T_c$ . Since the carbon generation requires large ensembles [5], it is expected that the amount of carbon deposited will decrease with increasing calcination temperature. In conclusion, the present study demonstrates that the structural properties and the reduction behavior and hence the catalytic performance of the MgO-supported Co catalysts are strongly affected by the heat treatment conditions.

## 4. Conclusion

The present investigation shows that many factors affect the structural and chemical properties of the MgO-supported Co catalysts. The structural changes are mainly induced by the tendency to form a solid solution between CoO and MgO. The formation of a solid solution is favored by high calcination temperatures and long calcination times. Eventually, a complete solid solution is generated. The impregnated catalysts show a stronger propensity to form a solid solution than the physically mixed ones, due to a higher initial dispersion of Co precursor over the support. The extent of solid solution formation has a pronounced effect on the catalyst reducibility and hence on its catalytic performance. It has been shown that the catalyst reducibility and its activity for carbon deposition in the  $\text{CH}_4$  decomposition became lower as the extent of solid solution increased.

## References

- [1] N. Elliott, J. Chem. Phys. 22 (1954) 1924.
- [2] P. Cossee, Mol. Phys. 3 (1960) 125.
- [3] C.N. Satterfield, in: *Heterogeneous Catalysis in Industrial Practice*, 2nd Ed. (McGraw-Hill, New York, 1991) (a) p. 400; (b) p. 420; (c) p. 433.
- [4] E. Ruckenstein and H.Y. Wang, Appl. Catal. A (2000), in press.
- [5] J.R. Rostrup-Nielsen, in: *Catalysis Science and Technology*, Vol. 5, eds. J.R. Anderson and M. Boudart (Springer, Berlin, 1984) pp. 1–118.